



OPEN

Smartphone based colorimetric approach for quantitative determination of uric acid using Image J

Samar H. Elagamy¹✉, Latifa Adly¹ & Mohamed Ahmed Abdel Hamid^{1,2}

Recently, significant attention has been directed towards digital image colorimetry DIC using mobile applications or available software programs, which offer the advantage of analyzing samples without the need for sophisticated instruments. One such image processing program is Image J, widely used for obtaining quantitative information from scientific images. Image J could measure the color intensities by quantifying of the RGB (red–green–blue) gray levels across the images of colored substances. These values are correlated to the color intensities through conversion to CMY (cyan–magenta–yellow) values which are proportional to the color intensities. The objective of this study is to develop an innovative analytical method for the quantitative determination of uric acid using Image J for color quantification. Image J was utilized to analyze images captured by smart phone for successive concentrations of uric acid that were previously treated with phosphotungstate to develop a blue color. The proposed method has been applied for determination of uric acid in real urine using standard addition method and the results were compared with UV/VIS spectrophotometry as a reference method. In this research, we will also assess the effectiveness of quantitative analysis using Image J in comparison to a mobile application, namely RGB Color Detector.

In the last few years, there has been a growing interest in incorporating image processing programs and mobile applications APPS into chemical analysis which permits green, fast and cost-effective analysis¹. These programs and AAPS have been utilized for colorimetry^{2,3}, fluorimetry⁴, chemiluminescence^{5,6} and electrochemical analysis⁷. Extensive research has been conducted on digital image colorimetry (DIC) as a versatile technique for both qualitative and quantitative analysis across various sample types including heavy metals⁸, pesticides^{9,10}, antibiotics¹¹, environmental samples¹² and food products^{13–15}. DIC is based on image acquisition with smartphone and color quantification using mobile APPS (RGB color detector, color meter, PhotoMetrix) or image processing programs (Adobe Photoshop, Image J, Matlab) under appropriate color system. The color quantification data were utilized to obtain analyte concentration¹⁶. Smartphones are preferable to digital cameras for image acquisition in DIC due to their portability, simplicity in use, significant improvement of camera functions, and the availability of mobile APPS^{17,18}.

Image J is an open-source image processing program designed by the national institutes of health NIH for analysis of scientific images. Image J has been extensively used in different biological studies include quantifying cellular and subcellular components¹⁹. It has also been successfully applied in analysis of various medical images including dental imaging, tumor differentiation, and brain tissue imaging^{20–22}. Image J offers several benefits compared to other image processing software such as the accessibility and ease of use of basic built in functions even without prior experience in image analysis. Furthermore, it has the capability to function on a wide range of computer platforms and possesses the ability to handle the majority of commonly used image formats. Image J functions include noise reduction, background subtraction, smoothing, sharpening, contrast manipulation, detection of regions of interest, and quantifying intensities. Additionally, it facilitates measurements of areas, volumes (stacks), distances, and angles^{23–25}.

Uric acid is a product of metabolic breakdown of purine (adenine and guanine) that exist in RNA and DNA Fig. 1. It is a weak acid with a pKa of 5.6 and it is sparingly soluble in water. The concentration of uric acid in serum and urine is an indicator of many renal complications. The normal uric acid concentration in urine is

¹Department of Pharmaceutical Analytical Chemistry, Faculty of Pharmacy, Tanta University, Tanta, Egypt. ²Department of pharmaceutical chemistry, Al Salam university, Tanta, Egypt. ✉email: samar.elagamy@pharm.tanta.edu.eg

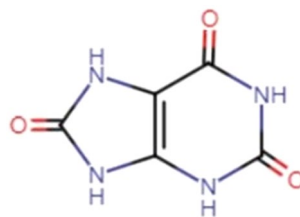


Figure 1. Chemical structure of uric acid.

250–750 mg/day. A high uric acid level (greater than 800 mg/day) can cause uric acid crystallization and deposition in joints, tendons and surrounding tissues and development of other medical conditions such as gout or urinary stones^{26,27}. Different chromatographic methods have been developed for determination of uric acid and creatinine in human urine^{28–30}. In addition, several colorimetric methods have been recently reported^{31–34}. In this study, we have applied DIC using Image J for quantitative determination of uric acid after treatment with phosphotungstate reagent in alkaline medium to develop a blue color. Image J was chosen for color quantitation as it outperforms mobile APPS in its capability to enable precise quantitative analysis, while mobile APPS is primarily suitable for qualitative or semi-quantitative analysis. This work is considered to be the first approach to use Image J as image processing program in DIC and the first investigation of the capabilities of image J in comparison to mobile APPS.

Materials and methods

Apparatus

Spectrophotometric measurements have been carried out using a Shimadzu (Japan) UV-1800 PC double beam spectrophotometer with 1 cm Quartz cells. UV probe software was used for spectra displaying and arithmetic calculations.

Materials

Uric acid, Sodium chloride NaCl, Sodium citrate $\text{Na}_3\text{C}_6\text{H}_5\text{O}_7 \cdot 2\text{H}_2\text{O}$, Sodium sulfate Na_2SO_4 , Magnesium sulfate $\text{MgSO}_4 \cdot 7\text{H}_2\text{O}$, Potassium chloride KCl, Potassium dihydrogen phosphate KH_2PO_4 were purchased from Fisher Scientific Company. Phosphotungstate reagent was kindly supplied from biochemistry department, faculty of pharmacy, Tanta university. Protein free urine sample collected over 24 hours was supplied from Elmenshawy hospital after the patient consent.

Preparation of artificial urine

Artificial urine was prepared by dissolving 1.5 gm Sodium chloride, 0.96 gm Potassium chloride KCl, 1.0982 gm Potassium dihydrogen phosphate, 1.0 gm Sodium citrate, 0.6 gm Sodium sulfate, and 0.1155 Magnesium sulfate in 250 mL distilled water³⁵. The pH of the prepared artificial urine was found to be 5.9.

Determination of uric acid in artificial urine

Uric acid stock solution ($30 \mu\text{g}\cdot\text{mL}^{-1}$) was prepared by dissolving 3.0 mg uric acid in diluted artificial urine 10:90 with distilled water DW. Different aliquots (1–5.0 mL) were quantitatively transferred into a series of 10 mL volumetric flask. 3.0 mL of Na_2CO_3 aqueous solution (10%) was added to each flask, and they were allowed to stand for 10 minutes. After that, 1.0 mL of folin reagent was added, mixed well using vortex and the volume was completed with DW to give final concentrations of $3.0\text{--}15 \mu\text{g}\cdot\text{mL}^{-1}$.

Determination of uric acid in real urine

10 mL of urine sample was diluted with 90 mL DW and the amount of uric acid in the sample was determined using standard addition method to eliminate the matrix effect through addition of different volumes (0.5, 1.0, 2.0, 3.0 mL) of uric acid standard solution ($30 \mu\text{g}\cdot\text{mL}^{-1}$) to 0.5 mL of diluted urine followed by the same procedure for color reaction under Section “[Determination of uric acid in artificial urine](#)”. The amount of uric acid in the real urine was calculated from the regression equation and then multiplied by dilution factor of 200:1 to obtain the initial concentration.

Imaging procedure

The serial dilutions of uric acid were placed in glass cuvettes and the images were captured using smart phone (Samsung Galaxy A52; 64 Mpx camera resolution), against white background in an imaging box in order not to be affected by daylight and to improve the signal to noise ratio². The images were cropped to remove blank spaces on all edges and brought together in one image with each segment representing a certain concentration Fig. 2a. The images were saved as TIFF (Tagged Image File Format). The average of the gray values was calculated for each segment.

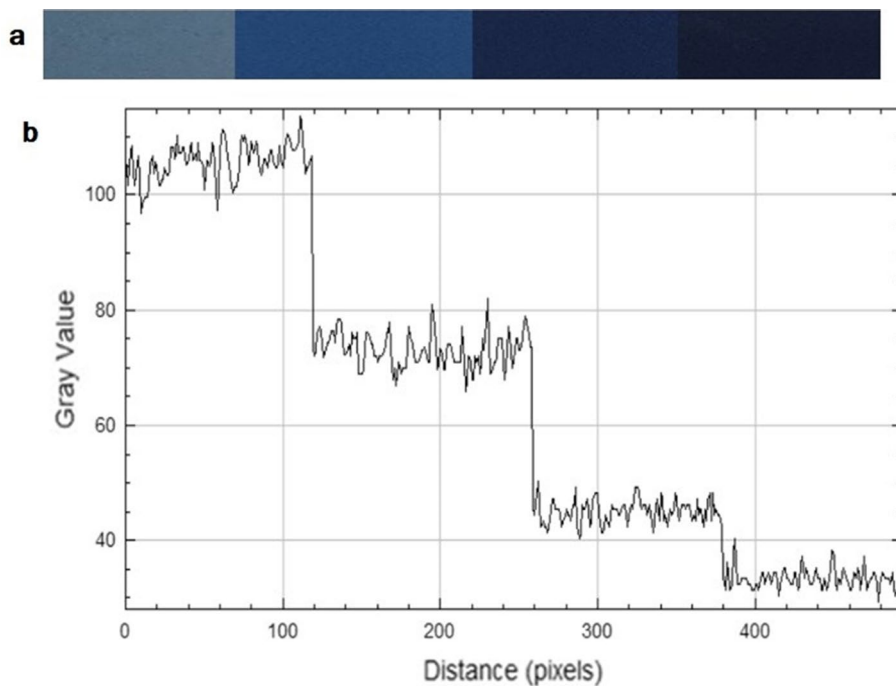


Figure 2. (a) The images of successive concentrations of uric acid (b) their corresponding gray value plot versus distance.

Results and discussion

In alkaline medium uric acid reduces phosphotungstate reagent producing tungsten blue color according to the Eq. 1²⁶



There is a linear relationship between the intensity of blue color and the concentration of uric acid. This was exploited to apply digital image colorimetry DIC using image J for color quantification. The RGB gray values were measured across the images of serial dilution of uric acid using image J and displayed as a plot of gray values versus the pixel positions. The RGB gray value is a numerical representation of the intensity of gray or color in a specific pixel, ranging from 0 (black) to 255 (white). This explains why in Fig. 2b, as depicted, the gray value increases with the reduction in color intensity. To establish a correlation between the RGB gray values and color intensity, they were transformed into complementary CMY (cyan–magenta–yellow) values using the formula CMY = 255 – RGB³⁶.

Optimization of experimental condition

All variables impacting the color reaction between uric acid and phosphotungstate were meticulously optimized to achieve an intense blue color and to maximize the absorbance value, consequently enhancing the method's sensitivity. The quantity of phosphotungstate reagent was subjected to examination, revealing that an optimal volume of 1.0 mL yielded the best results (see Fig. S1). Similarly, the influence of sodium carbonate amount was investigated, and the peak absorbance was attained with 3.0 mL of sodium carbonate (see Fig. S2). Furthermore, an optimum vortex time following the addition of the reagent was found to be 10 min (see Fig. S3). Table 1 summarizes all the factors affecting the color intensity and their optimal values.

Factors	Studied range	Effect	Optimum conditions
Volume of phosphotungstate reagent	0.2–2.0 mL	Increasing the volume results in increasing the color intensity followed by subsequent decrease	1.0 mL
Volume of sodium carbonate	1.0–5.0 mL	Increasing the volume results in increasing the color intensity then it remain unchanged	3.0 mL
Vortex time	3–15 min	Increasing the time results in increasing the color intensity then it remains constant	10 min

Table 1. Factors affecting the color intensity.

Comparison with a mobile application

For the assessment of the analytical performance of DIC using Image J, the color quantification was performed using a commonly used mobile application, RGB Color Detector alongside with a spectrophotometer. The mobile application RGB Color detector enables the analysis in four colour spaces—RGB, HSL, HSV, and HSI. The results are generated across eight channels, encompassing R, G, B, H, S, L, V, and I. The measurements were carried out across all channels, and ultimately, channel B was selected for optimal results since the color of the solutions changed from blue to black-blue and the increase in blue values with increasing the blue color intensity was significant Fig. 3.

Analytical characteristics of the proposed method

The calibration curve for DIC/Image J was constructed by plotting a relation between the CMY values derived from the images versus the uric acid concentration in diluted artificial urine while, for DIC/RGB analysis, the calibration curve was plotted using B values. For spectrophotometry, the absorbance values at λ_{max} of 700 nm were utilized. Figure S4 shows the absorption spectrum of the blue colored product. The calibration curves were found to be linear over the range $3.0\text{--}15 \mu\text{g}\cdot\text{mL}^{-1}$ Fig. 4. The study revealed that the correlation coefficient for DIC/Image J and spectrophotometry is nearly equivalent. However, the correlation coefficient for DIC/RGB showed a lower value of 0.97. The regression equations for all the methods were computed from the corresponding calibration curve. The regression parameters were listed in Table 2.

Limit of quantitation and limit of detection

The Limit of detection LOD and limit of quantitation LOQ values were calculated according to the following equations:

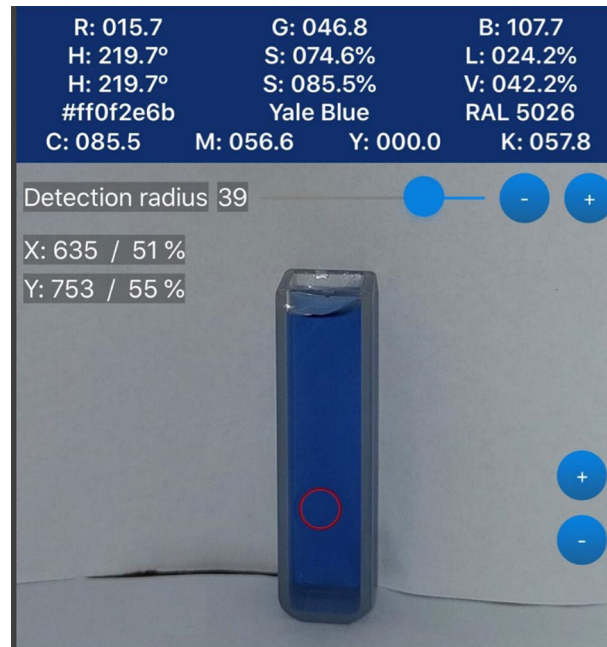


Figure 3. The measurement of color intensity using RGB color detector.

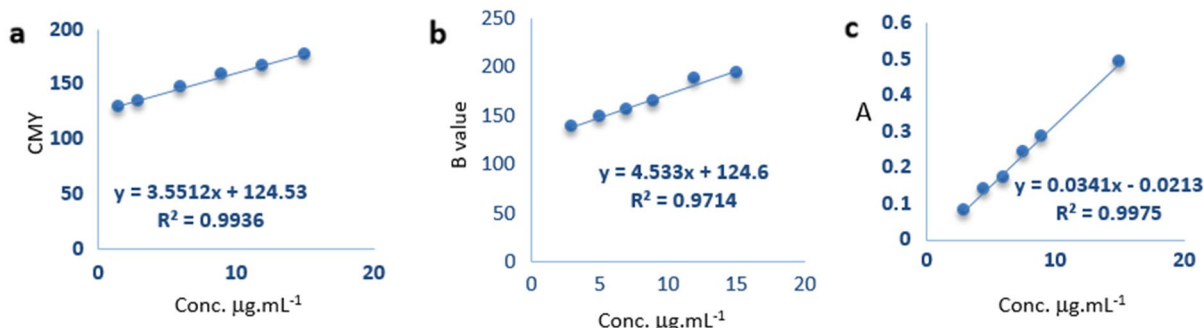


Figure 4. The calibration curves for (a) DIC/Image J, (b) DIC/RGB, and (c) spectrophotometry.

Parameters	DIC /Image J	DIC /RGB	Spectrophotometry
Concentration range $\mu\text{g}\cdot\text{mL}^{-1}$	3.0–15	3.0–15	3.0–15
Limit of detection LOD $\mu\text{g}\cdot\text{mL}^{-1}$	1.199	3.748	0.504
Limit of quantitation LOQ $\mu\text{g}\cdot\text{mL}^{-1}$	3.63	11.35	1.53
Regression parameters			
Slope \pm SD (Sb)	3.551 ± 0.142	4.533 ± 0.5497	0.034 ± 0.00066
Intercept \pm SD (Sa)	124.53 ± 1.29	124.6 ± 5.149	0.0204 ± 0.0052
SD of residual (Sxy)	1.666	4.878	0.00732
Correlation coefficient (r)	0.994	0.9714	0.999

Table 2. Regression parameters for colorimetric determination of uric acid.

$$\text{LOD} = 3.3\sigma/\text{Slope}$$

$$\text{LOQ} = 10\sigma/\text{Slope}$$

Where σ is the standard deviation of intercept.

The LOD value achieved with DIC/ Image J was comparable to UV–Vis spectrophotometry, whereas the LOD for DIC/ RGB was apparently higher.

Accuracy and precision

The accuracy was verified through the determination of five different concentrations of standard uric acid over the linearity range. The intra-day precision was performed through replicate analysis of five different concentrations of standard uric acid. Inter-day precision was tested by repeated analysis of five different concentrations of uric acid for a period of three successive days. The percent relative error (%RE) was computed for the purpose of method verification and evaluation of the bias between the stated concentration and the measured concentration. It is evident that DIC/Image J exhibit exceptional precision (RSD < 2%) and accuracy (100.39% recovery), comparable to spectrophotometry. On the other hand, the precision and accuracy results from the mobile application are generally lower, yet they remain within an acceptable range. However, at concentrations of $3.0 \mu\text{g}\cdot\text{mL}^{-1}$, the mobile application yielded less accurate and precise results. This indicates that DIC/RGB can be applied adequately for semi-quantitative analysis, while precise and accurate quantitative analysis can be achieved using DIC/Image J. The results of accuracy and precision are listed in Tables 3 and 4.

Actual Conc. $\mu\text{g}\cdot\text{mL}^{-1}$	DIC/Image J			DIC/RGB			Spectrophotometry		
	%Recovery	%RE	Mean %recovery*	%Recovery	%RE	Mean %recovery*	%Recovery	%RE	Mean %recovery*
3	98.116	1.884	100.099	95.09	4.91	98.37	100.83	0.83	100.241
6	101.46	1.46		97.52	2.48		100.38	0.38	
9	100.6	0.61		98.76	1.24		100.07	0.07	
12	100.46	0.46		99.23	0.77		99.954	0.046	
15	99.86	0.14		99.78	0.22		99.97	0.03	

Table 3. Evaluation of the accuracy for determination of uric acid. *Average of three determinations.

DIC/Image J			DIC/Image J			Spectrophotometry		
Intraday		Interday	Intraday		Interday	Intraday		Interday
Conc. Taken $\mu\text{g}\cdot\text{mL}^{-1}$	Mean Conc. found*	%RSD	Mean Conc. found*	%RSD	Mean Conc. found*	%RSD	Mean Conc. found*	%RSD
3	3.126	1.4	3.198	1.86	2.82	4.87	2.79	5.09
6	6.208	1.34	6.23	1.73	5.78	2.87	5.75	3.09
9	9.081	0.857	9.08	0.947	8.86	1.89	8.54	1.36
12	11.97	0.76	12.23	0.87	12.65	1.74	12.76	1.98
15	15.09	0.35	15.2	0.45	14.89	1.2	14.56	1.43

Table 4. Evaluation of the precision for determination of uric acid. *Average of three determinations.

Stability

The examination of the stability of the blue color formed was conducted over 30 min. The investigation revealed that the blue color remains stable for the initial 10 min, after which its intensity gradually diminishes Fig. 5. Consequently, all measurements were promptly performed immediately following the reaction to get optimal results.

Standard addition method

The standard addition method was employed for determination of uric acid in real urine to eliminate the matrix effect. The CMY and the absorbance values for the sample were determined from the intercept values of the curves and the concentration was calculated from the regression equations derived from the corresponding calibration curves Figure S5. The results for DIC show that the sample has a concentration of approximately $7.0 \text{ } \mu\text{g}\cdot\text{mL}^{-1}$ and the initial concentration of $1400 \text{ } \mu\text{g}\cdot\text{mL}^{-1}$ which were similar to spectrophotometry. This indicates the capability of DIC for accurate determination of uric acid in real samples.

Greenness assessment

The greenness of DIC Method was assessed using Analytical Greenness metric AGREE calculator. This assessment involves 12 principles of green analytical chemistry that are transformed into a standard scale of 0–1 scale reflecting the greenness of the method. The pictogram for AGREE calculator has twelve sections with the total score in the center. The color of each section range from dark green (= 1) to dark red (= 0) based on the ecological impact³⁷. The DIC method allows at line and instantaneous analysis of the samples thus it achieved a score of 0.76. Table 5 shows the assessment of AGREE and the adherence of the developed method to the 12 principles of green analytical chemistry, presenting corresponding scores for each principle. Figure 6 represents the pictograms for AGREE metrics for DIC.

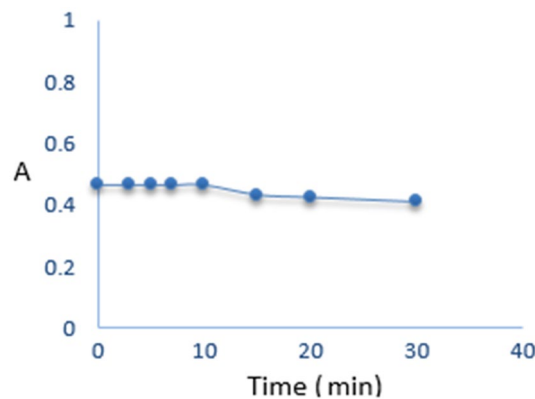


Figure 5. Study of the stability of the blue colored product for $12.0 \text{ } \mu\text{g}\cdot\text{mL}^{-1}$ uric acid.

Principle	Comment	Score
Principle 1: Sample Pretreatment Activities	Sample pretreatment such acid deproteinization and treatment with phosphotungstate	0.3
Principle 2: Minimal Sample Size	Sample size 10mL	1
Principle 3: In Situ Measurements	At line analysis(little or no sample pretreatment, sample preservation is avoided and preservation agents are not needed)	0.33
Principle 4. Integration of Analytical Processes and Operations Saves Energy and Reduces the Use of Reagents	3 steps or fewer	1
Principle 5. Automated and Miniaturized Methods	Manual and not miniaturized	0
Principle 6. Derivatization	Phosphotungstate reagent (CAS 51312-42-6)	0.8
Principle 7. Generation of a Large Volume of Analytical Waste Should Be Avoided and Proper Management of Analytical Waste Should Be Provided	Waste volume = 10 mL	0.39
Principle 8. Multianalyte or Multiparameter Methods	One analyte at a time	0.94
Principle 9. The Use of Energy Should Be Minimized	Non-instrumental detection (smartphone-based analysis)	1
Principle 10. Reagents Obtained from Renewable Source Should Be Preferred	None of the reagents are bio based	0
Principle 11. Toxic Reagents Should Be Eliminated or Replaced	None of the reagents are toxic	1
Principle 12. The Safety of the Operator Should Be Increased	None of the reagents are flammable or corrosive	1

Table 5. The report for AGREE assessment.



Figure 6. AGREE pictogram for DIC.

Comparison with other reported colorimetric method

Our research presents a distinctive approach for uric acid determination compared to other reported methods as shown in Table 6. The penalty points pps for all reagents and solvents utilized in these methods were calculated as the following³⁸.

$$\text{The hazard} = \text{signal word} * \text{number of hazard pictograms}$$

Where signal word danger = 2pps, warning = 1pps.

The first reported method relies on a complexion reaction involving uric acid, potassium ferricyanide, and ferric chloride in a hydrochloric acid medium HCl which is known for its corrosiveness and irritant properties³¹. Furthermore, two other reported methods involve the utilization of metal-organic framework MIL-53(Fe) and WO_3 Nanosheets. Despite their high sensitivity, the synthesis of these materials is complex, time-consuming, and necessitates the use of non-green solvents, along with requiring extensive chemical and physical characterization^{32,34}. Another method involving silver nanoparticles, while simpler and faster than the former two, still involves multiple procedures, non ecofriendly reagents, and characterization steps³³. In contrast, our proposed method stands out for its use of green reagents, its one-step reaction process, and non-instrumental determination of color intensity, making it energy-efficient and environmentally friendly. Thus, our approach offers a practical alternative with satisfactory linearity range while addressing the complexities associated with other reported methods.

Colorimetric method principle	Linearity range	Sample	Detection mode	Comment	Reagents	References
Complexion with potassium ferricyanide, and ferric chloride	2–200 $\mu\text{g}\cdot\text{mL}^{-1}$	Urine and serum	Blue colored complex measured at maximum wavelength 752 nm	–	HCl pps = 2 (signal word danger and one hazard pictogram) Potassium ferricyanide pps* = 2 (warning and two pictogram) Ferric chloride pps = 4 (danger and two pictogram)	³¹
MIL-53 Fe as a colorimetric sensor	0.75–10 $\mu\text{g}\cdot\text{mL}^{-1}$ (4.5–60 μM)	Urine and serum	Blue colored product measured at maximum wavelength 652 nm	Synthesis of this metal organic frame work requires heating for 17 h and 24 h drying	Solvent DMF pps = 6 (danger and three pictogram) Ferric chloride pps = 4	³²
AgNPs as a colorimetric sensor	0.0168 $\text{ng}\cdot\text{mL}^{-1}$ 16.8 $\mu\text{g}\cdot\text{mL}^{-1}$ (0.1 nM–0.1 mM)	Spiked serum samples	Color change of the solution from brown to yellow. In parallel, the absorbance is blue shifted from 477 to 428 nm	Synthesis of silver nanoparticles require stirring for 1 h at 95 °C	Silver nitrate pps = 6 (danger and three pictogram)	³³
WO_3 NSs as a colorimetric sensor	0.33–30 $\mu\text{g}\cdot\text{mL}^{-1}$ (2–180 μM)	Serum	Blue color measured at maximum wavelength 652 nm	Synthesis of nano sheets require magnetic stirring for 72 h and drying for 12 h	Sodium tungsten oxide dihydrate ($\text{Na}_2\text{WO}_4\cdot 2\text{H}_2\text{O}$) pps* = 1 (warning and one pictogram) Solvent HNO_3 pps* = 2 (danger and one pictogram)	³⁴
Phosphotungstate	3–15 $\mu\text{g}\cdot\text{mL}^{-1}$	Urine	Blue color measured using DIC/Image J	Phosphotungstate reagent pps = 1 (warning and one pictogram)	Our proposed method

Table 6. Comparison with other reported colorimetric methods.

Conclusions

This study clearly demonstrates the feasibility of utilizing DIC/Image J for determining uric acid levels in both artificial and real urine samples. This approach offers the advantage of easy monitoring of uric acid without the need for any specialized instruments. Additionally, the use of Image J offers good analytical parameters, at the same time it is uncomplicated and the analysis can be performed directly without the need for numerous trials to determine the optimal channel, as required with mobile APPS. This study also proves that, Image J can be employed for accurate and precise quantitative analysis whereas mobile APPS prove satisfactory for semi-quantitative analysis. Notably this colorimetric approach using Image J has a great potential for various other applications, including colorimetric determination of heavy metals or drug analysis utilizing specific reagents. Overall, this novel method presents a promising avenue for diverse analytical tasks with a smartphone-based approach.

Data availability

All data generated or analyzed during this study are included in this published article (and its Supplementary Information files).

Received: 20 August 2023; Accepted: 1 December 2023

Published online: 11 December 2023

References

- El-Shaheny, R., Al-Khateeb, L. A. & El-Maghrebey, M. Dual-excitation in-lab-made device based on a handy UV lamp and GQDs-modified PADs for simultaneous determination of acetaminophen and its endocrine disrupting impurity 4-nitrophenol. *Sens. Actuators B Chem.* **348**, 130657 (2021).
- Chen, G. *et al.* Improved analytical performance of smartphone-based colorimetric analysis by using a power-free imaging box. *Sens. Actuators B Chem.* **281**, 253–261 (2019).
- Hassan, R. O., Othman, H. O. & Ali, D. S. New spectrophotometric and smartphone-based colorimetric methods for determination of atenolol in pharmaceutical formulations. *Spectrochim. Acta Part A Mol. Biomol. Spectrosc.* **302**, 123009 (2023).
- Larsen, T. & Moyes, K. M. Fluorometric determination of uric acid in bovine milk. *J. Dairy Res.* **77**, 438–444 (2010).
- Shahvar, A., Saraji, M. & Shamsaei, D. Smartphone-based chemiluminescence sensing for TLC imaging. *Sens. Actuators B Chem.* **255**, 891–894 (2018).
- Zangheri, M. *et al.* A simple and compact smartphone accessory for quantitative chemiluminescence-based lateral flow immunoassay for salivary cortisol detection. *Biosens. Bioelectron.* **64**, 63–68 (2015).
- Scott, A. *et al.* A smartphone operated electrochemical reader and actuator that streamlines the operation of electrochemical biosensors. *ECS Sens. Plus* **1**, 14601 (2022).
- Sivakumar, R. & Lee, N. Y. Recent progress in smartphone-based techniques for food safety and the detection of heavy metal ions in environmental water. *Chemosphere* **275**, 130096 (2021).
- Tang, Y. *et al.* Facile colorimetric smartphone-based biosensor for rapid detection of organophosphorus pesticides residues in environment using the aptamer-enhanced oxidase activity of octahedral Ag₃O particles. *Anal. Chim. Acta* **1264**, 341325 (2023).
- Zhao, T. *et al.* Smartphone-based colorimetric sensor array using gold nanoparticles for rapid distinguishment of multiple pesticides in real samples. *Food Chem.* **404**, 134768 (2023).
- Cao, F.-J., Cheng, H.-H., Ma, S.-X., Jiao, F. & Dong, D.-M. Three-channel smartphone-based aptamer sensor for multiplexed detecting antibiotics in water through resonance light scattering. *Sens. Bio-Sensing Res.* **38**, 100533 (2022).
- Vargas-Muñoz, M. A., Morales, J., Cerdà, V., Ferrer, L. & Palacio, E. Paper sensor-based method using a portable 3D-printed platform and smartphone-assisted colorimetric detection for ammonia and sulfide monitoring in anaerobic digesters and wastewater. *Microchem. J.* **188**, 108469 (2023).
- Yam, K. L. & Papadakis, S. E. A simple digital imaging method for measuring and analyzing color of food surfaces. *J. Food Eng.* **61**, 137–142 (2004).
- Resende, L. M. B., Magalhães, E. J. & Nunes, C. A. Optimization and validation of a smartphone-based method for the determination of total sterols in selected vegetable oils by digital image colorimetry. *J. Food Compos. Anal.* **117**, 105111 (2023).
- Peng, B. *et al.* A smartphone-based colorimetry after dispersive liquid–liquid microextraction for rapid quantification of calcium in water and food samples. *Microchem. J.* **149**, 104072 (2019).
- Kiliç, V., Horzum, N. & Solmaz, M. E. From sophisticated analysis to colorimetric determination: Smartphone spectrometers and colorimetry. *Color Detect.* 1–19 (2018).
- Fan, Y., Li, J., Guo, Y., Xie, L. & Zhang, G. Digital image colorimetry on smartphone for chemical analysis: A review. *Measurement* **171**, 108829 (2021).
- Rezazadeh, M., Seidi, S., Lid, M., Pedersen-Bjergaard, S. & Yamini, Y. The modern role of smartphones in analytical chemistry. *TrAC Trends Anal. Chem.* **118**, 548–555 (2019).
- Lam, J. *et al.* A universal approach to analyzing transmission electron microscopy with ImageJ. *Cells* **10**, 2177 (2021).
- Yan, H. *et al.* Imaging brain tumor by dendrimer-based optical/paramagnetic nanoprobe across the blood-brain barrier. *Chem. Commun.* **47**, 8130–8132 (2011).
- Geiger, M., Blein, G. & Ludwig, A. Evaluation of ImageJ for relative bone density measurement and clinical application. *J. Oral Heal. Craniofacial Sci.* **1**, 12–21 (2016).
- Lee, H.-W. *et al.* Breast tumor classification of ultrasound images using wavelet-based channel energy and imageJ. *IEEE J. Sel. Top. Signal Process.* **3**, 81–93 (2009).
- Hartig, S. M. Basic image analysis and manipulation in ImageJ. *Curr. Protoc. Mol. Biol.* **102**, 14–15 (2013).
- Lind, R. Open source software for image processing and analysis: Picture this with ImageJ. In *Open Source Software in Life Science Research* (eds Harland, L. & Forster, M.) 131–149 (Elsevier, 2012).
- Ferreira, T. & Rasband, W. ImageJ user guide ImageJ/Fiji 1.46. *Revis. Ed. ImageJ* (2012).
- Kumar, V., Gill, K. D., Kumar, V. & Gill, K. D. To determine the uric acid concentration in serum and urine (2018).
- Fathallah-Shaykh, S. A. & Cramer, M. T. Uric acid and the kidney. *Pediatr. Nephrol.* **29**, 999–1008 (2014).
- Zhou, S. *et al.* An eco-friendly hydrophilic interaction HPLC method for the determination of renal function biomarkers, creatinine and uric acid, in human fluids. *Anal. Methods* **5**, 1307–1311 (2013).
- Jen, J.-F., Hsiao, S.-L. & Liu, K.-H. Simultaneous determination of uric acid and creatinine in urine by an eco-friendly solvent-free high performance liquid chromatographic method. *Talanta* **58**, 711–717 (2002).
- Wijemanne, N., Soysa, P., Wijesundara, S. & Perera, H. Development and validation of a simple high performance liquid chromatography/UV method for simultaneous determination of urinary uric acid, hypoxanthine, and creatinine in human urine. *Int. J. Anal. Chem.* **2018**, 1647923 (2018).

31. Al-kadumi, A. S. H., Abdulsattar, J. O. & Nabhan, K. J. Colorimetric determination of uric acid in live samples. *Indian J. Forensic Med. Toxicol.* **14**, 1120–1127 (2020).
32. Lu, J., Xiong, Y., Liao, C. & Ye, F. Colorimetric detection of uric acid in human urine and serum based on peroxidase mimetic activity of MIL-53 (Fe). *Anal. Methods* **7**, 9894–9899 (2015).
33. Li, L., Wang, J. & Chen, Z. Colorimetric determination of uric acid based on the suppression of oxidative etching of silver nanoparticles by chloroauric acid. *Microchim. Acta* **187**, 1–7 (2020).
34. Yang, J. *et al.* Spectrophotometric detection of uric acid with enzyme-like reaction mediated 3, 3', 5, 5'-tetramethylbenzidine oxidation. *Bull. Chem. Soc. Ethiop.* **37**, 11–21 (2023).
35. Brown, P., Ackermann, D. & Finlayson, B. Calcium oxalate dihydrate (weddellite) precipitation. *J. Cryst. Growth* **98**, 285–292 (1989).
36. Islam, M. N., Ahmed, I., Anik, M. I., Ferdous, M. S. & Khan, M. S. Developing paper based diagnostic technique to detect uric acid in urine. *Front. Chem.* **6**, 496 (2018).
37. Pena-Pereira, F., Wojnowski, W. & Tobiszewski, M. AGREE—Analytical GREENness Metric Approach and Software. *Anal. Chem.* **92**, 10076–10082 (2020).
38. Gałuszka, A., Migaszewski, Z. M., Konieczka, P. & Namieśnik, J. Analytical Eco-Scale for assessing the greenness of analytical procedures. *TrAC Trends Anal. Chem.* **37**, 61–72 (2012).

Author contributions

S.E. and L.A. conducted the experiments. M.A.H. analyzed the results, assisted in writing, and revising the manuscript. All authors reviewed the manuscript.

Funding

Open access funding provided by The Science, Technology & Innovation Funding Authority (STDF) in cooperation with The Egyptian Knowledge Bank (EKB).

Competing interests

The authors declare no competing interests.

Additional information

Supplementary Information The online version contains supplementary material available at <https://doi.org/10.1038/s41598-023-48962-0>.

Correspondence and requests for materials should be addressed to S.H.E.

Reprints and permissions information is available at www.nature.com/reprints.

Publisher's note Springer Nature remains neutral with regard to jurisdictional claims in published maps and institutional affiliations.



Open Access This article is licensed under a Creative Commons Attribution 4.0 International License, which permits use, sharing, adaptation, distribution and reproduction in any medium or format, as long as you give appropriate credit to the original author(s) and the source, provide a link to the Creative Commons licence, and indicate if changes were made. The images or other third party material in this article are included in the article's Creative Commons licence, unless indicated otherwise in a credit line to the material. If material is not included in the article's Creative Commons licence and your intended use is not permitted by statutory regulation or exceeds the permitted use, you will need to obtain permission directly from the copyright holder. To view a copy of this licence, visit <http://creativecommons.org/licenses/by/4.0/>.

© The Author(s) 2023